Inorganic Chemistry
ARTICLE
pubs.acs.org/IC

Facile Synthesis of Zero-, One-, and Two-Dimensional Vanadyl Pyrophosphates

Diego Solis-Ibarra,[†,‡] Jared S. Silvia,[†] Vojtech Jancik,[‡] and Christopher C. Cummins*,[†]

[†]Department of Chemistry, Massachusetts Institute of Technology, 77 Massachusetts Avenue, Cambridge, Massachusetts 02139, United States

[‡]Centro Conjunto de Investigación en Química Sustentable UAEM-UNAM, Carr. Toluca-Atlacomulco Km 14.5, Unidad San Cayetano C.P. 50200, Toluca, Edo. de México, México

S *Supporting Information*

ABSTRACT: Crystallization of $Na_2VOP_2O_7$ from its aqueous solution results in formation of a one-dimensional inorganic polymer $\{Na_2VO(H_2O)P_2O_7 \cdot 7H_2O\}_n$ (**1**). When this polymer is dehydrated at elevated temperatures this polymer undergoes a phase transition to form the two-dimensional framework β-$Na_2VOP_2O_7$, which although previously reported had been difficult to access. Exchanging lithium for sodium via ion-exchange chromatography results in formation of a discrete, cyclic, tetramer species, $Li_8[VOP_2O_7(H_2O) \cdot 4H_2O]_4$ (**2**). Isolation of crystalline β-$Li_2VOP_2O_7$ using a dehydration procedure analogous to the one employed for the sodium derivative was unsuccessful. In contrast, we show that β-$K_2VOP_2O_7$ can be obtained from the amorphous phase $K_2VOP_2O_7 \cdot nH_2O$ (n = 0−7) upon thermal dehydration.

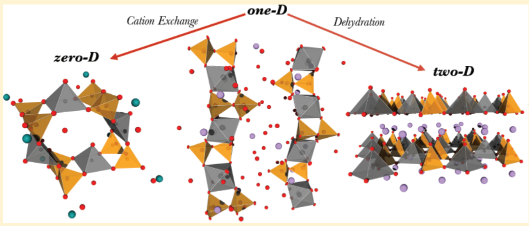

INTRODUCTION

Investigations into the chemistry of vanadyl pyrophosphates have been motivated by their catalytic and biological relevance. This family of compounds includes the only commercial catalyst for selective oxidation of butane to maleic anhydride (vanadium−phosphorus−oxide, VPO or $VOPO_4$)[1] and insulin-mimetic compounds relevant to diabetes research.[1a,2] To date, structural studies of these materials have been performed on samples obtained from solid-state, high-temperature syntheses and crystallizations. Alternatively, organic compounds such as HTMP (2,4,6-trimethylpyridinium),[3] methoxy groups,[3] or bipyridine[4] have been used as supporting ligands, countercations, and/or crystallization enhancers.

On the other hand, the aqueous behavior of the pyrophosphate and vanadyl ions has been investigated extensively; early studies by Rieger and co-workers determined the solution structure of sodium vanadyl pyrophosphate to be a cyclic trimer, $[Na_2VOP_2O_7]_3$,[5] which was later confirmed by means of electronic, infrared, and Raman spectroscopies.[6] No further attempts at structural characterization or isolation have been documented. Thus, we initially sought to isolate and fully characterize this compound in order to study its potential as a catalyst for oxidation reactions. Herein, we describe the synthesis and characterization of a new series of vanadyl pyrophosphates, three of which were prepared using simple benchtop procedures, without using solvothermal methods or even high-temperatures synthesis. These compounds were found to exhibit a fascinating cation-dependent structural diversity.

EXPERIMENTAL SECTION

General Considerations. Aqueous solutions were prepared using reagent-grade deionized water ($r \geq 18$ MΩ/cm; Ricca Chemical Co., USA). Organic solvents were reagent grade or better and not dried prior to use. Commercially available reagents, including $Na_4P_2O_7 \cdot 10H_2O$, $K_4P_2O_7$, LiCl (Aldrich), and $OVSO_4 \cdot 2H_2O$ (Strem), were used as received. High-temperature syntheses were performed in a Lindberg furnace (model 51894).

High-resolution electrospray ionization mass spectrometry (ESI-MS) was performed using a Bruker Daltonics APEXIV 4.7 T Fourier Transform Ion Cyclotron Resonance Mass Spectrometer (FT-ICR-MS). Qualitative elemental analyses were performed using energy-dispersive X-ray spectroscopy (view Supporting Information for experimental conditions and images). Quantitative elemental analyses were performed by Midwest Microlab, LLC, Indianapolis, IN.

Synthesis of $\{Na_2VO(H_2O)P_2O_7 \cdot 7H_2O\}_n$ (1). An aqueous solution of $OVSO_4 \cdot 2H_2O$ (1.00 g; 1.50 mmol) in 20 mL of H_2O was slowly added to an aqueous solution of $Na_4P_2O_7 \cdot 2H_2O$ (0.67 g; 1.50 mmol in 20 mL of H_2O). After 2 h of stirring, THF (80 mL) was added. After agitation, the mixture was allowed to settle until an oily, deep blue gel was formed in the bottom of the flask. The supernatant liquid was decanted away from the blue phase using a separatory funnel. The blue gel was then washed with 20 mL of a mixture of water/THF (30:70). The oily suspension was then diluted with water (5 mL), and then in a 100 mL Erlenmeyer flask approximately 30 mL of THF was carefully layered on top of the blue phase. After 3 days, the THF had diffused into

Received: March 11, 2011
Published: September 21, 2011

the aqueous phase and compound **1** crystallized on the botton of the flask. After decanting the mother liquid away from the crystals, compound **1** was obtained in 82% yield (0.53 g; 1.23 mmol). Single crystals of **1** suitable for X-ray diffraction studies were found among the crystalline product. Crystalline **1** readily loses water with concomitant loss of crystallinity. Therefore, **1** should be kept in the presence of the mother liquor to maintain its crystalline form. Alternatively, **1** can be dried to obtain amorphous $\mathbf{1}\cdot n\mathrm{H_2O}$ (Figure 1S, Supporting Information), where the value of "n" depends on the drying procedure, with n values between zero and seven ($n = 0-7$).

High-resolution negative ESI-MS results are as follows. Found, 837.5009 m/z; calcd for $[\mathrm{Na_5(OVP_2O_7)_3}]^-$, 837.5012. Anal. Calcd for $\mathrm{Na_2V(O)P_2O_7\cdot 8\,H_2O}$: P, 14.37; H, 3.74. Found: P, 14.59; H, 3.58.

Synthesis of β-$\mathrm{Na_2V(O)P_2O_7}$ (1β). Crystalline **1** was dried overnight under vacuum. After this procedure, amorphous $\mathbf{1}\cdot n\mathrm{H_2O}$ was obtained. Repeated thermogravimetric analyses (TGA) determined the hydration state to be $n = 3.12$. These solids were loaded into an alumina crucible (1.00 g, 2.91 mmol) and heated using a 5 °C/min ramp up to 500 °C and then held at that temperature for an additional 60 min. After controlled cooling (−10 °C/min), green crystallites (0.78 g, 2.68 mmol) of pure **1β** were obtained in 93% yield.[7] Formation of **1β** was corroborated trough PXRD and SEM-EDX (see Supporting Information).

Synthesis of $\mathrm{Li_8[VOP_2O_7(H_2O)\cdot 4H_2O]_4}$ (2). A solution of $\mathrm{OVSO_4\cdot 2H_2O}$ (0.45 g; 2.23 mmol) in water (15 mL) was added dropwise to a solution of $\mathrm{Na_4P_2O_7\cdot 10H_2O}$ (1.00 g; 2.24 mmol) in water (15 mL). The reaction mixture was stirred for 1 h, after which time THF was added (10 mL). After agitation, an intense blue gel-like product was formed in the bottom of the flask. This gel was loaded into a 1 × 25 cm column of Dowex 1 × 4 (200 mesh) ion-exchange resin in the $\mathrm{Cl^-}$ form (after it had been washed with 1.0 M LiCl, followed by pure $\mathrm{H_2O}$ immediately before use). A 1 M solution of LiCl was used as the eluent. Once the first fraction eluted, the eluent was changed to 1.5 M LiCl. The second (and major) fraction was then collected. This fraction was concentrated using the rotovap and subsequently washed with an acetone/water mixture (ca. 1:10 water/acetone) until no LiCl was observed. Ultimately, by carefully layering acetone on top of an aqueous solution of **2**, 0.255 g of $\mathrm{Li_8[VOP_2O_7(H_2O)\cdot 4H_2O]_4}$ crystallites was obtained for a final yield of 33% (7.40 mmol). From among the obtained solids, some crystals of **2** suitable for single-crystal X-ray diffraction studies were harvested.

High-resolution negative ESI-MS results are as follows. Found, 502.7473 m/z; calcd for $[\mathrm{Li_6(OVP_2O_7)_4}]^{2-}$: 502.7496. Anal. Calcd for $\mathrm{Li_2V(O)P_2O_7\cdot 5H_2O}$: P, 17.96; H, 2.90. Found: P, 17.99; H, 2.92.

Synthesis of β-$\mathrm{K_2V(O)P_2O_7}$ (3β). A solution of $\mathrm{OVSO_4\cdot 2H_2O}$ (2.40 g, 12.00 mmol in 20 mL of water) was slowly added to a solution of $\mathrm{K_4P_2O_7}$ (4.00 g; 12.00 mmol in 40 mL) in water at ambient temperature. The reaction mixture was stirred for 1 h. After that, THF was slowly added until a blue precipitate was formed. This precipitate was filtered and washed several times with THF/water mixtures (50:50). After drying under vacuum, a light blue powder was obtained. This powder was then loaded into an alumina crucible, heated in a furnace using a 5 °C/min ramp up to 550 °C, and then held at that temperature for 2 h. After controlled cooling (−10 °C/min), green crystallites of **3β** were obtained in 76% yield (2.91 g; 9.12 mmol). Formation of **3β** was corroborated through PXRD and SEM-EDX (see Supporting Information).

Single-Crystal X-ray Diffraction Studies. Low-temperature diffraction data for compound **1** and **2** were collected on a Bruker D8 three-circle diffractometer coupled to a Bruker-AXS Smart Apex CCD detector with graphite-monochromated Cu Kα radiation ($\lambda = 1.54178$ Å). In both cases φ and ω scans were performed. The structures were solved by direct methods using SHELXS and refined against F^2 on all data by full-matrix least-squares with SHELXL-97[8] following established refinement strategies.[9] All non-hydrogen atoms were refined anisotropically. Coordinates for hydrogen atoms bound to oxygen were located in the difference Fourier synthesis and subsequently refined semifreely with the help of distance restraints. Isotropic displacement parameters of all hydrogen atoms were fixed to 1.5 times the U value of the atoms they are linked to. Details regarding the data quality and a summary of the residual values of the refinements are listed in Table 1.

Table 1. Crystallographic Data for Compounds 1 and 2[a]

compound	1	2
empirical formula	$\mathrm{H_{16}Na_2O_{16}P_2V}$	$\mathrm{H_{20}Li_8O_{42}P_8V_4}$
fw, g·mol $^{-1}$	430.99	1199.21
temperature, K	100(2)	100(2)
wavelength, Å	1.54178	1.54178
cryst syst	monoclinic	monoclinic
space group	$P2_1/n$	$C2/m$
a, Å	8.7852(1)	18.3531(4)
b, Å	9.6094(1)	14.0324(3)
c, Å	16.7847(3)	11.9795(3)
α, deg	90	90
β, deg	98.571(1)	130.007(1)
γ, deg	90	90
volume, Å^3	1401.15(3)	2363.14(9)
Z	4	2
density (calc), g/cm^3	2.043	1.685
abs coeff, mm^{-1}	9.539	9.975
$F(000)$	876	1185
goodness-of-fit on F^2	1.228	1.116
final R indices [$I > 2\sigma(I)$]	$R_1{}^b = 0.0365$, $wR_2{}^c = 0.\,0908$	$R_1{}^b = 0.0679$, $wR_2{}^c = 0.1792$
R indices (all data)	$R_1{}^b = 0.0366$, $wR_2{}^c = 0.0910$	$R_1{}^b = 0.0725$, $wR_2{}^c = 0.1821$

[a] Complete crystallographic tables, CIF files, and details regarding the refinement of both structures can be found in the Supporting Information. [b] $R_1 = \Sigma||F_o| - |F_c||/\Sigma|F_o|$. [c] $wR_2 = [\Sigma w(F_o{}^2 - F_c{}^2)^2/\Sigma(F_o{}^2)^2]^{1/2}$.

Both structures presented disordered water molecules and $\mathrm{H_2O\cdots V{\equiv}O}$ moieties (see Supporting Information for further details in refinement of **2**). Disorders were refined using similarity restraints on 1,2 and 1,3 distances and displacement parameters as well as rigid bond restraints for anisotropic displacement parameters. The ratios between the components of all disorders were refined freely while constraining the sum of the occupancies to unity. Similar rigid-bond restraints were also applied to atoms not involved in disorders to stabilize the refinement.

Powder X-ray Diffraction (PXRD). Experiments were conducted at the MIT Center for Materials Science and Engineering (CMSE) X-ray facility using a Panalytical X'Pert Pro diffractometer with a Bragg—Brentano geometry and High Speed X'Celerator Detector (see Supporting Information, Table 2S, for further information regarding the experiment and instrumental details). Variable-temperature powder X-ray diffraction (VT-PXRD) experiments were carried out using an Anton Paar HTK-1200N oven. Measurements were carried out with constant flow of nitrogen gas over the sample. The heating program was such that after initial data collection at room temperature the sample was heated to 100 °C and then in steps of 25 °C until a temperature of 650 °C was reached. Before each experiment, a 10 min delay was introduced to ensure equilibrium conditions. All PXRD data was analyzed using X'pert HighScore Plus Program.[10] Theoretical powder patterns were calculated using the crystallographic information files (*.cif) obtained from the Inorganic Chemistry Structural Database (**1β** and **3β**) or from single-crystal X-ray experiments (**1** and **2**).

Thermogravimetric and Calorimetric analyses. Thermogravimetric analyses (TGA) and differential scanning calorimetry (DSC)

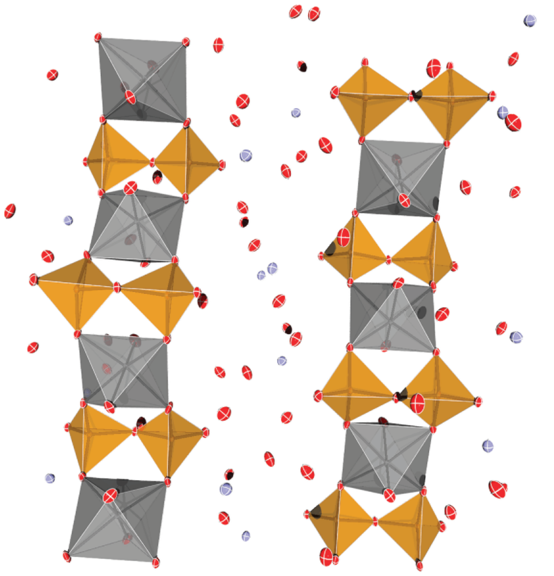

Figure 1. Polyhedral-ellipsoid representation of **1** viewed along the *a* axis and with hydrogen atoms omitted for clarity. Displacement ellipsoids are drawn at the 40% probability level. Color code: V = gray, P = orange, O = red, Na = purple.

were performed in the Materials Research Science and Engineering Center at Harvard University using TA Q5000 and Q200 Instruments, respectively. Unless otherwise noted, samples were usually between 5 and 15 mg weight and heated in a platinum (TGA) or aluminum pan (DSC) under argon (TGA) or nitrogen (DSC) flow with a heating ramp of 10 °C/min up to 550 °C.

RESULTS AND DISCUSSION

Compound $Na_2VOP_2O_7$ was prepared from reaction of sodium pyrophosphate with vanadyl sulfate in aqueous media. Use of vanadyl perchlorate (resembling Parker's original procedure)[5] does not affect the results described hereafter. When THF was allowed to slowly diffuse into a concentrated aqueous solution of $Na_2VOP_2O_7$, light blue, prismatic crystals were obtained in 83% yield. Such crystals could also be obtained by diffusion of acetonitrile into an aqueous solution of $Na_2VOP_2O_7$ or very slow evaporation of an aqueous solution of $Na_2VOP_2O_7$. Regardless of the crystallization method, crystals obtained were suitable for single-crystal X-ray studies and determined to be a polyhydrate of the compound: $\{Na_2VO(H_2O)P_2O_7 \cdot 7H_2O\}_n$ (**1**). In all cases, the crystals exhibit identical cell parameters and feature compound **1** in the monoclinic space group $P2_1/n$, accompanied by eight water molecules per vanadium atom (Figure 1).

Compound **1** adopts an unexpected one-dimensional polymeric motif with $[(H_2O)VOP_2O_7]_n$ chains running along the *b* axis. The vanadyl ion is situated in a distorted octahedral coordination environment comprised of two bidentate pyrophosphate ligands in the equatorial positions and a water molecule and the vanadyl oxo group in the axial positions. The oxo groups of adjacent vanadium centers point in alternating directions and are involved in an extensive hydrogen-bonding network together with the interstitial water molecules coordinated to the sodium countercations. The solid structure differs from the previously reported trimeric solution structure of this compound.[5,6] We suggest that **1** undergoes a depolymerization−polymerization process when going from solution to the solid state and vice versa.

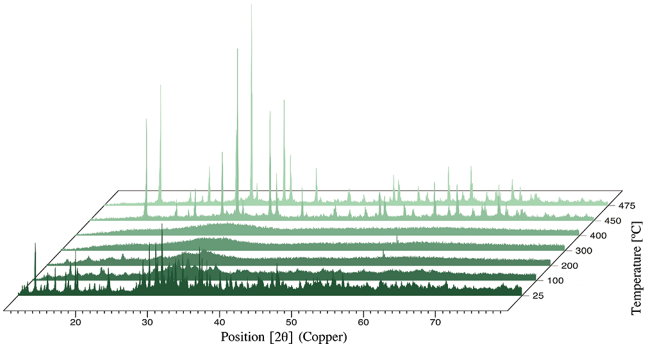

Figure 2. Variable-temperature powder X-ray diffraction study of crystalline **1**. Only selected runs are plotted for clarity.

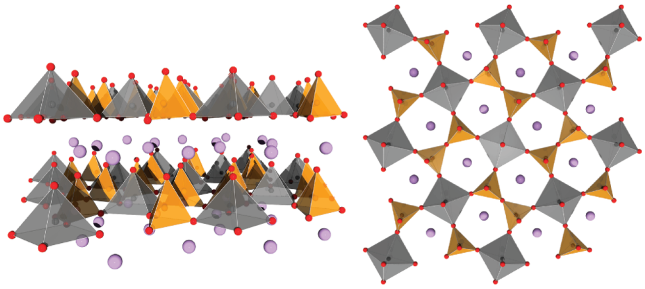

Figure 3. Polyhedral representation of **1*β*** along the *b* (left) and *c* (right) axes. Color code: V = gray, P = orange, O = red, Na = purple. Created from the crystallographic information file downloaded from the Inorganic Crystal Structure Database (ICSD, reference code 50376).

Therefore, cyclic trimers should predominate in solution, while the polymeric structure is limited to the solid state. This hypothesis is supported by negative-ion ESI-MS, which contained no fragment heavier than $[Na_5(OVP_2O_7)_3]^-$, and from the reluctance of crystalline **1** to redissolve in water.[11]

Upon manipulation, crystals of **1** readily lose water with concomitant loss of crystallinity. Nevertheless, powder X-ray diffraction (PXRD) studies confirmed that the bulk of the product corresponds to the same crystal system found in the single-crystal experiment (Figure 1). Furthermore, while attempting to quantify the amount of water in the isolated solid using thermogravimetric analysis (TGA), it was observed that the light blue powder turned irreversibly into green crystallites. This observation led us to conduct a variable-temperature powder X-ray diffraction (VT-PXRD) experiment that revealed a phase transition at approximately 450 °C (Figure 2).

The resulting dehydration product was identified as the previously reported β-polymorph of **1**, β-$Na_2VOP_2O_7$ (**1*β***).[12] Pralong and co-workers reported that compound **1*β*** is difficult to access based upon unsuccessful attempts to isolate this phase.[13] Nevertheless, our procedure can be easily scaled up to multigram quantities with use of a conventional furnace. From a molecular perspective, this transformation is even more notable as it involves a condensation reaction in which the one-dimensional chains ostensibly fuse to form two-dimensional layers. The vanadium ions go from a six-coordinate, octahedral environment to a five-coordinate, square-pyramidal mode, and all of the vanadyl moieties realign to point in the same direction, perpendicular to the sheets. The pyrophosphate groups rearrange to bridge four different vanadium atoms each, shifting from a μ_2- to a μ_4-bridging mode (Figure 3).

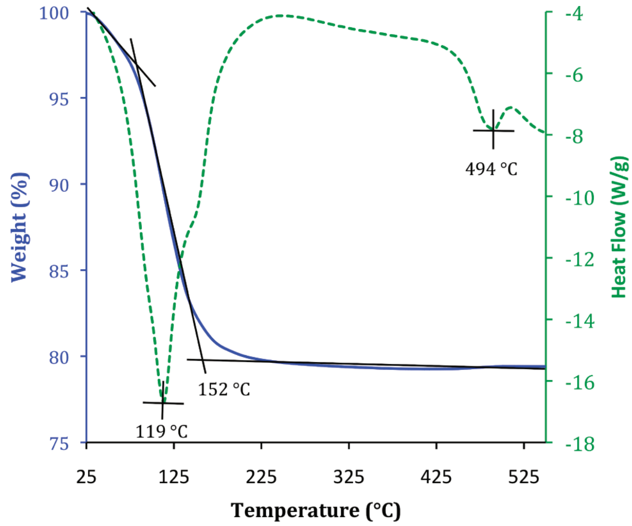

Figure 4. Thermogravimetric analysis (blue/solid) and differential scanning calorimetry (green/dashed) of $Na_2V(O)P_2O_7 \cdot nH_2O$. The first peak in the DSC (119 °C) corresponds to the dehydration step, whereas the second peak (494 °C) is related to the phase transition.

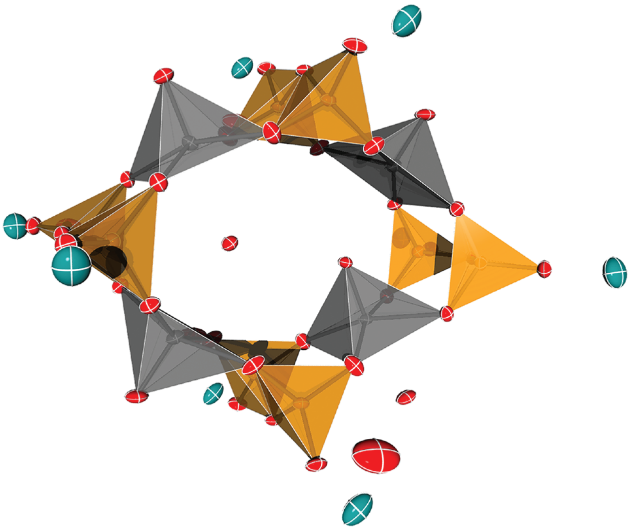

Figure 5. Polyhedral-ellipsoid representation of **2** with hydrogen atoms omitted for clarity. Displacement ellipsoids are drawn at the 40% probability level. Color code: V = gray, P = orange, O = red, Li = aqua.

The mechanism of this transformation has yet to be determined, but thermogravimetric studies (TGA) and differential scanning calorimetry (DSC) experiments have shown that the phase transition is not coupled to the dehydration process (Figure 4).

After these initial synthetic studies, we became interested in extending this work to other cations, particularly lithium. Transition metal phosphates that contain lithium are of interest as solid materials for development of more efficient batteries; this is one of the keystones in the contemporary renewable energy revolution.[14] In fact, the lithium analogue of **1*β***, *β*-$Li_2VOP_2O_7$, has been considered as a potential cathode material for Li-ion batteries.[13] In the present work, $Li_2VOP_2O_7$ was obtained from **1** by passing an aqueous solution of the latter through an ion-exchange resin using LiCl as the eluent.[13]

After recrystallization from water layered with acetone, light blue crystalline $Li_8[VOP_2O_7(H_2O) \cdot 4H_2O]_4$ (**2**) was obtained in moderate yield. Among the obtained solids, some crystals of **2** were suitable for single-crystal X-ray diffraction studies.[15] Interestingly, the crystal structure of **2** is not analogous to the corresponding sodium derivative **1**. Instead, **2** adopts a zero-dimensional structure with a closed circular tetrameric core $[Li_2VOP_2O_7(H_2O)]_4$. Three of the four vanadyl moieties are pointed outward, while the remaining vanadyl unit points inward and hydrogen bonds to an included water molecule (Figure 5). This water molecule is weakly coordinated to the vanadyl ions as evidenced by the $V-OH_2$ distances, which range between 2.446(6) and 2.476(5) Å and are notably longer than the corresponding $V-OH_2$ distance found in **1** (2.308(1) Å). As corroborated by TGA, compound **2** crystallizes with five molecules of water per vanadium atom. Two and a half of the five water molecules are located within large voids of the crystal (276 and 267 $Å^3$, respectively); thus, we were not able to obtain a stable refinement for these water molecules due to high positional disorder.[16]

Combustion analysis and PXRD studies confirmed that the bulk of the product from the cation exchange is complex **2**, and it shares its composition and structure with the one elucidated by single-crystal diffraction methods. To the best of our knowledge, there is no crystallographic precedent for this structural motif of pyrophosphate groups serving as the only bridging ligand between metals to form a wheel structure. The contrast between the solid-state structures of **1** and **2** may be explained by the difference in the size of the cations affecting the cation coordination number (and therefore hydration level) and the ability of the pyrophosphate groups to come within proximity of one another, thus accounting for the structural differences between **1** and **2**. At the moment, it is unclear whether the tetrameric structure of **2** persists in solution. However, the negative-ion ESI-MS exhibits a peak at 502.7473 *m*/*z* which is in close agreement with the theoretical value for $[Li_6(VOP_2O_7)_4]^{2-}$ (502.7496 *m*/*z*), thereby suggesting that this is indeed the case.

Attempts to obtain *β*-$Li_2VOP_2O_7$ (**2*β***) by means of high-temperature dehydration proved to be unsuccessful. A VT-PXRD experiment revealed that thermolysis of **2** results in formation of lithium vanadyl orthophosphate ($LiVOPO_4$) as well as other unidentified products. Further attempts to synthesize crystalline **2*β***, including a procedure analogous to the one used in the isolation of *α*-$Li_2VOP_2O_7$[13] from *α*-$Na_2VOP_2O_7$, were also futile.

Although we were unable to isolate a crystalline hydrated form of $K_2OVP_2O_7$ (**3**), we observed that when amorphous $\mathbf{3} \cdot nH_2O$[17] was heated at 550 °C for 1 h *β*-$K_2OVP_2O_7$ (**3*β***), which is isostructural with **1*β***,[18] is produced cleanly. This observation represents a significant improvement in the synthesis of **3*β***, because previous methodologies required the use of higher temperatures (860 °C) and longer periods of time (12 h).[18] Furthermore, we we were able to confirm that it is possible to obtain **1*β*** from amorphous $Na_2V(O)P_2O_7 \cdot nH_2O$ under similar conditions.

In conclusion, we developed mild synthetic protocols for several vanadyl pyrophosphates that can be produced in large quantities from commercially available and inexpensive reagents without the need for solvothermal methods and in some cases without the need of high temperatures. Furthermore, we have shown that solid-state structures of anionic vanadyl pyrophosphates are highly dependent on the countercation and hydration state, both of which are responsible for significant conformational changes.

ASSOCIATED CONTENT

Supporting Information. Complete experimental details, full crystallographic information and CIF files, as well as additional single-crystal, PXRD, SEM-EDX, and TGA pictures. This material is available free of charge via the Internet at http://pubs.acs.org.

AUTHOR INFORMATION

Corresponding Author
*E-mail: ccummins@mit.edu.

ACKNOWLEDGMENT

This work was funded by the NSF CCI program (grant NSF CHE-0802907). D.S. gratefully acknowledges the financial support by Consejo Nacional de Ciencia y Tecnología (Beca Mixta and project No. 79531). This work made use of the MRSEC Shared Experimental Facilities at MIT, supported by the National Science Foundation under award number DMR-08-19762. Anthony F. Cozzolino, Scott A. Speakman, and Glen E. Alliger are also acknowledged for crystallographic assistance. The MRSEC program of the National Science Foundation under Award Number DMR-08-20484 provided TGA and DSC instrumentation.

REFERENCES

(1) (a) Ikotun, O. F.; Marino, N.; Kruger, P.; Julve, M.; Doyle, R. *Coord. Chem. Rev.* **2010**, *254*, 890–915. (b) Martin, A.; Bentrup, U.; Wolf, G. *Appl. Catal., A* **2002**, *227*, 131–142. (c) Koo, H.; Whangbo, M.; VerNooy, P.; Torardi, C.; Marshall, W. *Inorg. Chem.* **2002**, *41*, 4664–4672. (d) Centi, G.; Trifiro, F.; Ebner, J. R.; Franchetti, V. M. *Chem. Rev.* **1988**, *88*, 55–80.

(2) (a) Yuen, V. G.; Orvig, C.; McNeill, J. H. *Am. J. Physiol.* **1997**, *272*, E30–35. (b) McNeill, J. H.; Tahiliani, A. *Trends Pharmacol. Sci.* **1986**, *7*, 364–367.

(3) Herron, N.; Thorn, D. L.; Harlow, R. L.; Coulston, G. W. *J. Am. Chem. Soc.* **1997**, *119*, 7149–7150.

(4) Doyle, R.; Nieuwenhuyzen, M.; Kruger, P. *Dalton Trans.* **2005**, *2005*, 3745–3750.

(5) Parker, C.; Reeder, R.; Richards, L.; Rieger, P. *J. Am. Chem. Soc.* **1970**, *92*, 5230–5231.

(6) Muglia, C.; Ferrer, E.; Baran, E. *J. Therm. Anal. Calorim.* **2001**, *65*, 177–183.

(7) The 7% yield loss is likely due to limitations in transferring solids.

(8) (a) Sheldrick, G. *SHELXL-97, program for crystal structure refinement*; University of Göttingen: Göttingen, 1997, (b) Sheldrick, G. M. *Acta Crystallogr., Sect. A* **2007**, *64*, 112–122.

(9) (a) Müller, P.; Herbst-Irmer, R.; Spek, A.; Schneider, T.; Sawaya, M.; Müller, P., *Crystal Structure Refinement: A Crystallographer's Guide to SHELXL*, 1st ed.; Oxford University Press: New York: 2006; p 232, (b) Müller, P. *Crystallogr. Rev.* **2009**, *15*, 57–83.

(10) *X'pert HighScore Plus Program*, Version 2.2; PAN'analytical: Almelo, The Netherlands, 2002.

(11) Dissolution is only possible after stirring overnight or sonicating suspensions.

(12) Daidouh, A.; Veiga, M.; Pico, C. *Solid State Ionics* **1998**, *106*, 103–112.

(13) Kishore, M. S.; Pralong, V.; Caignaert, V.; Varadaraju, U. V.; Raveau, B. *Solid State Sci.* **2008**, *10*, 1285–1291.

(14) (a) Armand, M.; Tarascon, J.-M. *Nature* **2008**, *451*, 652–657. (b) Nishimura, S.-i.; Nakamura, M.; Natsui, R.; Yamada, A. *J. Am. Chem. Soc.* **2010**, *132*, 13596–13597. (c) Cheng, F.; Tao, Z.; Liang, J.; Chen, J. *Chem. Mater.* **2008**, *20*, 667–681.

(15) It is also possible to obtain such crystals by carefully layering THF or acetonitrile onto an aqueous solution of **2**. Regardless of the crystallization method the same crystalline system was observed every time.

(16) (a) van der Sluis, P.; Spek, A. *Acta Crystallogr., Sect. A* **1990**, *46*, 194–201. (b) Spek, A. *J. App. Crystallogr.* **2003**, *36*, 7–13.

(17) $n = 0-7$ depending on the drying procedure.

(18) Gorbunova, Y. E.; Linde, S. A.; Lavrov, A. V.; Tananaev, I. V. *Dokl. Akad. Nauk. SSSR* **2010**, *250*, 350–353.